

*Short Communication*

## **Fabrication of ZnO/Polypyrrole/Carbon Nanotube Nanocomposite and its Application for Removal of 4-Chlorophenol from Wastewater**

Hong Xing\*, Changwei An, Lihong Wu, Yanguang Xu

Department of Biomedical and Chemical Engineering, Liaoning Institute of Science and Technology, Benxi 117004, Liaoning, P. R. China

\*E-mail: [xxinggg68@sina.com](mailto:xxinggg68@sina.com)

Received: 6 January 2021 / Accepted: 1 March 2022 / Published: 5 April 2022

---

The present work demonstrates a facile solution method for the preparation of ZnO/polypyrrole/carbon nanotube (ZnO/PPy/CNTs) nanocomposite as an effective photocatalyst for the degradation of 4-Chlorophenol (4-CP) from industrial wastewater under irradiation with UV and simulated sunlight. Structural and morphological characterizations using XRD and SEM illustrated the successful formation of ZnO/PPy/CNTs nanocomposite. EIS analysis showed that ZnO/PPy/CNTs with the low charge transfer resistance, can improve the interfacial photogenerated carrier transfer rate. Optical studies of samples using UV-vis absorption spectra indicated that the optical band gaps of ZnO, ZnO/PPy and ZnO/PPy/CNTs were estimated ~3.39, 3.30 and 3.17 eV, respectively, and the values of the optical band gap of ZnO decreased slightly as PPy and CNTs were added to the ZnO structure. The complete degradation of 100 ml of 6 mg/l 4-CP in water for ZnO, ZnO/PPy and ZnO/PPy/CNTs was obtained after 160, 140 and 120 minutes of exposure to UV light, and after 150, 120 and 100 minutes of exposure to simulated sunlight, respectively. The results showed that ZnO/PPy/CNTs exhibited the effective performance for photodegradation of 4-CP under simulated sunlight because of positive synergistic effect of PPy and CNTs on the light harvesting ability of ZnO. Study of the capability of the ZnO/PPy/CNTs for degradation of 4-CP in the prepared real sample of textile wastewater showed the proposed photocatalyst can effectively be used for the degradation of 4-CP from industrial wastewater.

---

**Keywords:** 4-Chlorophenol; ZnO; polypyrrole/CNTs nanocomposite; photodegradation

### **1. INTRODUCTION**

4-Chlorophenol (4-CP) or p-Chlorophenol, also known 4-hydroxychlorobenzene has a strong phenol odor and is one of the most toxic phenolic compounds [1, 2]. 4-CP is used as an intermediate for the synthesis of chlorinated chemicals, pesticides, pharmaceuticals, and dyes [3-5]. These phenolic

compounds are potentially persistent and recalcitrant toxicants that are widely spread in the environment and may cause health and environmental problems, especially contaminating industrial wastewater and leading to aquatic life problems. 4-CP as a toxic organic material has the potential to cause histopathological changes, mutagenic, and carcinogenic effects [6-8]. It has negative effect on the central nervous system and studies have indicated that it weakens the central nervous system and causes restlessness and headaches and, in severe cases, seizures, coma [9-11]. It causes damage to the kidneys, liver and pancreas [12-14].

Thus, many studies have been conducted on removing the 4-CP from contaminated industrial wastewaters using DC corona discharge plasma [15], electro-Fenton [16], photo-Fenton process [17], reverse osmosis [18], anodic oxidation [19], coagulation processes [20], and photodegradation [21-26]. Between these methods, the photodegradation process, as a low-cost method, uses semiconductors such as TiO<sub>2</sub> and ZnO as well as light as an energy source to the oxidative destruction of organic contaminants in water [27-29].

However, problems such as high recombination rates of photogenerated charge carriers and low utilization of solar energy have been observed in photocatalytic systems [30-32]. Studies have shown that the use of nanocomposites and heterostructure photocatalysts can overcome these problems. Therefore, the present work presented a facile solution method for the preparation of ZnO/PPy/CNTs nanocomposite as an effective photocatalyst for the degradation of 4-CP from wastewater under irradiation with UV and simulated sunlight.

## 2. EXPERIMENTAL

### 2.1. Preparation ZnO/PPy/CNTs nanocomposite

A facile solution method was used for the preparation of ZnO/PPy/CNTs nanocomposite [33]. 100 ml of 0.2 M NaOH (99%, Shandong Energy Chemical Co., Ltd., China) was gradually mixed with 50 ml of 0.2 M Zinc nitrate (98%, Shandong Energy Chemical Co., Ltd., China) solution and the resulted mixture was continuously stirred for 5 hours at 65 °C to obtain ZnO as white precipitate. Then, the products were washed with ethanol (99%, Shandong Energy Chemical Co., Ltd., China) and deionized water, respectively. The product was transferred into oven and dried at 65 °C. Following that, 100 mg of the resulting ZnO powder was mixed with 4 mg of PPy (99%, Shandong Energy Chemical Co., Ltd., China), 4 mg of CNTs (90%, Shandong Energy Chemical Co., Ltd., China), and 100 ml of deionized water for 60 minutes before being mildly sonicated. The resultant precipitate was separated by decantation, and transferred into an oven to dry at 65 °C.

### 2.2. Characterization

A scanning electron microscope (SEM) and an X-ray diffractometer were used for morphological and crystallographic analyses of samples. A UV–vis spectrophotometer was used to record the UV–visible absorption spectra of samples. An electrochemical impedance spectroscopy

(EIS) experiment was carried out using Autolab potentiostat-galvanostat with a three-electrode system containing ZnO or ZnO based nanocomposites (ZnO/PPy and ZnO/PPy/CNTs) as the working electrode, platinum wire as the counter electrode, and an Ag/AgCl as the reference electrode. These measurements were performed under simulated sunlight in an electrolyte solution of 0.5 M Na<sub>2</sub>SO<sub>4</sub> (99%, Shandong Energy Chemical Co., Ltd., China) in the frequency range from 10<sup>-2</sup> Hz to 10<sup>5</sup> Hz at open circuit potential.

### 2.3. Study photocatalytic degradation

The photocatalytic degradation performance of ZnO, ZnO/PPy and ZnO/PPy/CNTs was investigated for the removal of 100 ml of 4-CP in water under dark conditions and the irradiation of UV light and simulated sunlight. A photoelectrocatalytic study was conducted in a test chamber that contained a photocatalyst and the 4-CP (≥90%, Shandong Energy Chemical Co., Ltd., China) solution, which was prepared with deionized water. Before exposure to light, the prepared 100 ml of 4-CP as test solution in the presence of photocatalysts was magnetically stirred for 1 hour in dark conditions at room temperature to ensure establishment of adsorption–desorption equilibrium. The photocatalyst amount in the 4-CP solution was 0.5 g/l. 500 W parallel xenon lamp (Xi'an Toption Instrument Co., Ltd., China) and Uvc Lamp (254nm, T8 G13 Uv, Haining Hualiang Lighting Appliance Co., Ltd., China) were applied to simulation of the sunlight and UV sources, respectively, which are located at the top of the device. The distance between the surface of the light source and the surface of solution was kept constant at 5 cm. An optical absorbance spectrum of samples was obtained using a UV–Vis diffuse reflectance spectrometer. Optical absorption spectra was recorded after light irradiation with a spectrophotometer ( $\lambda_{\max} = 225$  nm, UV/V UNICO SQ-2800) [21]. Photodegradation efficiency ( $\eta$ ) of photocatalysts to remove the pollutant was determined by equation (2) [34, 35]:

$$\eta (\%) = \frac{C_0 - C_t}{C_0} \times 100 = \frac{A_0 - A_t}{A_0} \times 100 \quad (2)$$

Where  $C_0$ ,  $A_0$ , and  $C_t$ ,  $A_t$  are the concentration and the corresponded absorbance intensity of the 4-CP at initial and after the photodegradation process at time  $t$ , respectively.

## 3. RESULTS AND DISCUSSION

### 3.1. Structural and morphological characterizations

The structural characterization of prepared CNTs, PPy/CNTs and ZnO/PPy/CNTs was investigated by XRD as depicted in Figure 1. XRD pattern of CNTs shows diffraction peak at 26.35° which related to (002) characteristic of graphitic plane of CNTs (JCPDS card files, no. 41–1487) [36, 37]. The XRD pattern of PPy/CNTs shows a broad and weak diffraction peak of (002) plane, indicating that the CNTs overlap with the amorphous PPy [38]. XRD pattern of ZnO/PPy/CNTs shows diffraction peaks at 31.68°, 34.37°, 36.28°, 47.42°, 56.50°, 62.70°, 67.73°, and 68.97° which

corresponded to (100), (002), (101), (102), (110), (103), (112), and (201) planes of hexagonal wurtzite phase of ZnO, respectively (JCPDS card files, no. 36–1451) [39–41], and additional weak diffraction peak of (002) plane of CNTs, illustrating to successful formation of nanocomposite.

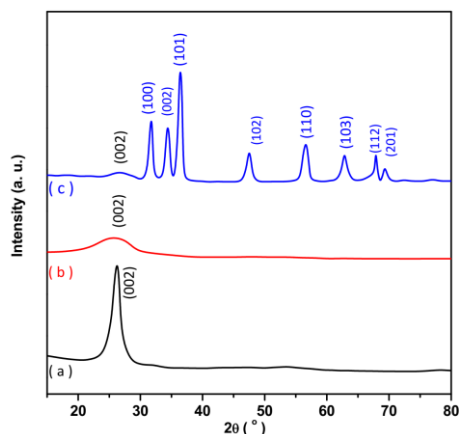


**Figure 1.** XRD pattern of (a) CNTs, (b) PPy/CNTs and (c) ZnO/PPy/CNTs

Figure 2 shows the SEM images of CNTs and ZnO/PPy/CNTs. SEM images of CNTs show typical views of the dense vertically aligned CNTs arrays with an average diameter of 95 nm. As observed from SEM images of ZnO/PPy/CNTs, ZnO nanoparticles are randomly distributed on the PPy/CNTs that significantly enhance the effective surface area and, thereby, electrocatalytic activity.

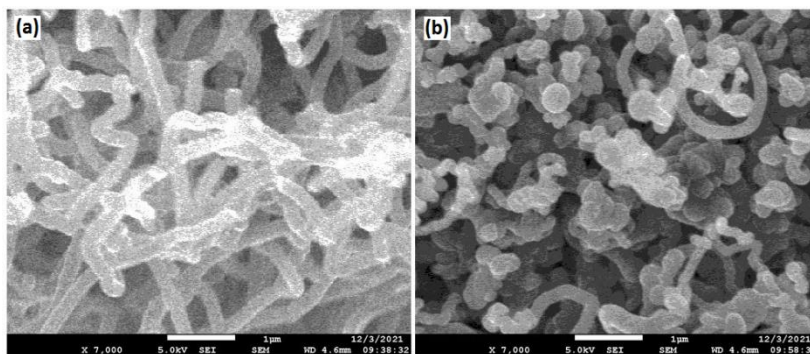


**Figure 2.** SEM images of (a) CNTs, (b) ZnO/PPy/CNTs.

### 3.3. EIS analysis

The EIS analysis was applied to study the impedance and separation of photogenerated carriers in photocatalysts. Figure 3 indicates the Nyquist plots, bode magnitude, phase angle plot and resultant equivalent circuit of ZnO, ZnO/PPy and ZnO/PPy/CNTs photocatalysts under simulated sunlight. Figure 3a shows a semicircle at high frequency, which corresponds to the interfacial charge transfer resistance [42–44], and smaller semicircle radius sizes correspond to less charge transfer resistance, better separation efficiency of photogenerated electrons, and more inhabitation for photogenerated electrons and holes recombination [45, 46]. Table 1 shows the parameter values for the equivalent

circuit model (Figure 3d) that was used to analyze the EIS data. The  $R_s$  is solution resistance,  $R_p$  and  $R_b$  are the resistances of the porous and barrier layers, which are associated with the charge transfer resistance through the nanostructured photocatalysts.  $Q_p$  and  $Q_b$  corresponds to the capacitances of the porous layer and barrier layer, which is related to the formation of the passive film layer on the electrode. The obtained result shows that the capacitance values  $Q_p$  and  $Q_b$  increase, and the resistances  $R_p$  and  $R_b$  decrease in ZnO/PPy/CNTs sample. Among all prepared photocatalysts, ZnO/PPy/CNTs show the lowest charge transfer resistance, and thereby the fastest interfacial photogenerated carriers transfer rate and prolonged life time of photogenerated electrons and holes at the interface of the nanocomposite [47-49].

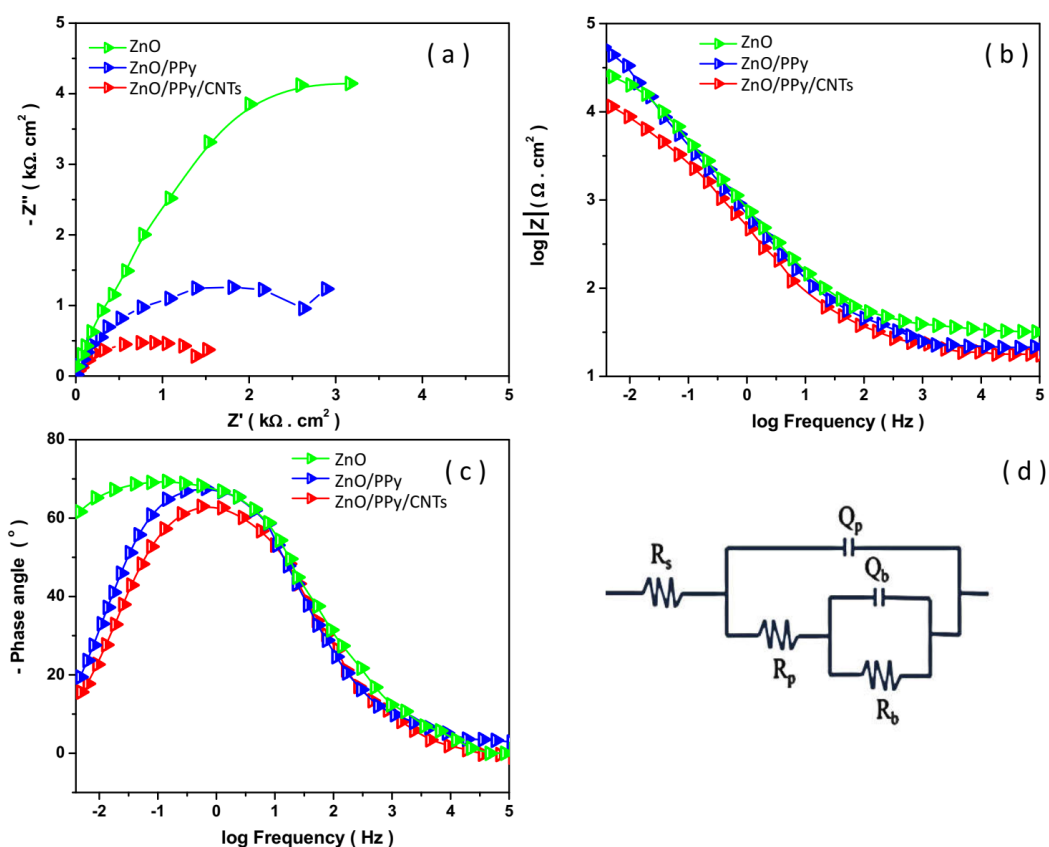


**Figure 3.** (a) Nyquist impedance plot, (b) Bode magnitude plot, (c) Bode phase plot and (d) the resulted equivalent circuit of ZnO, ZnO/PPy and ZnO/PPy/CNTs photocatalyst under simulated sunlight in electrolyte solution of 0.5 M Na<sub>2</sub>SO<sub>4</sub> in the frequency range from 10<sup>-2</sup> Hz to 10<sup>5</sup> Hz at open circuit potential.

**Table 1.** The resulted values for fitting data of the circuit elements.

| Sample       | $R_s$ ( $\Omega \cdot \text{cm}^2$ ) | $R_p$ ( $\Omega \cdot \text{cm}^2$ ) | $R_b$ ( $\Omega \cdot \text{cm}^2$ ) | $Q_p$ ( $\mu\text{F} \cdot \text{cm}^2$ ) | $Q_b$ ( $\mu\text{F} \cdot \text{cm}^2$ ) | $N_p$ | $N_b$ |
|--------------|--------------------------------------|--------------------------------------|--------------------------------------|---|---|-------|-------|
| ZnO          | 43.21                                | 74.31                                | 176                                  | 0.22                                      | 0.33                                      | 0.76  | 0.87  |
| ZnO/PPy      | 30.10                                | 46.40                                | 32                                   | 1.18                                      | 0.23                                      | 0.73  | 0.85  |
| ZnO/PPy/CNTs | 20.01                                | 39.78                                | 12                                   | 0.31                                      | 0.17                                      | 0.70  | 0.82  |

### 3.3. Optical study of samples

The optical properties of the ZnO, ZnO/PPy and ZnO/PPy/CNTs nanoparticles were studied using UV–vis absorption spectroscopy, as displayed in Figure 4a. As seen, the light absorption intensities of ZnO/PPy and ZnO/PPy/CNTs toward the ZnO are remarkably increased and the absorption edges are slightly red-shifted which can be related to the fact that the addition of PPy and CNTs introduces the intermediate energy level to reduce the energy of absorbed light [50]. In addition, the rough surface of ZnO/PPy/CNTs enhances the scattering path of incident light [51, 52]. As a consequence, it can improve the light absorption performance. The band gap of samples can be determined using Kubelka's formula [53]:

$$(\alpha h\nu) = A(h\nu - E_g)^{1/2} \quad (2)$$

Where  $h\nu$  and  $\alpha$  are photon energy and absorption coefficient, respectively.  $A$  is the proportionality constant and  $E_g$  is the optical band gap. The  $E_g$  could be determined by extrapolation of the linear curve to zero absorption edge energy, corresponding curve between  $(\alpha h\nu)^2$  and  $h\nu$  is also called the Tauc plot [54]. As observed from Figure 4b, the  $E_g$  of ZnO, ZnO/PPy and ZnO/PPy/CNTs are estimated  $\sim 3.39$ , 3.30 and 3.17 eV, respectively, which is in good agreement with literature values [55-57]. It is observed that the values of the  $E_g$  decrease slightly with the addition of PPy and CNTs in the ZnO structure, indicating an improvement in the conductivity of the nanostructure due to the effect of PPy as conductive polymer and CNTs [58]. Therefore, with increasing the conductivity the  $E_g$  is decreased which can be also attributed to the formation of new intermediate energy levels between valence band and conduction band because of the addition of PPy and CNTs [59]. Thus, electron started moving from the valence band to the conduction band through intermediate level. It accelerates the charge separation and transport at the ZnO/PPy/CNTs interface, as well as effectively improving the internal electron density [60]. This change reduces the recombination of photogenerated electron-hole pairs and enhances the absorption of solar radiation by decreasing the  $E_g$  value and broadening the light response range [58, 59, 61].

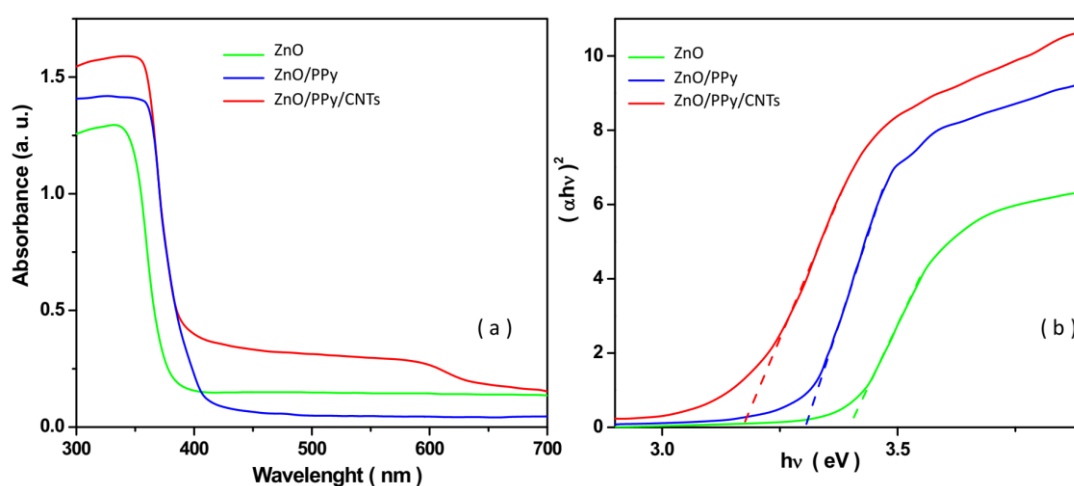


**Figure 4.** (a) UV–vis absorption spectra of the ZnO, ZnO/PPy and ZnO/PPy/CNTs nanoparticles and (b) related Tauc plots

### 3.4. Study the photocatalytic performance

Figure 5a shows the  $\eta$  of ZnO, ZnO/PPy and ZnO/PPy/CNTs for the removal of 100 ml of 6 mg/l 4-CP in water under dark conditions (first 45 minutes) and UV light irradiation. After 45 minutes in the dark, no significant degradation (1%) was observed. After 60 minutes of exposure to UV light, the remarkable photodegradation is observed and  $\eta$  values for ZnO, ZnO/PPy and ZnO/PPy/CNTs are determined as 75.1, 82.3 and 90.8%, respectively. After 160, 140, and 120 minutes of UV light exposure, complete degradation of ZnO, ZnO/PPy, and ZnO/PPy/CNTs is obtained, respectively. The achieved results imply that the greater photocatalytic activity is obtained for ZnO/PPy/CNTs nanocomposite that is associated with collaboration of the PPy/CNTs composite with the ZnO nanostructure and suppression of photogenerated carriers by anchoring ZnO nanoparticles onto PPy and CNTs, and generation of Zn-O-C bonds [62]. Many studies have been also reported in ZnO/CNTs nanocomposites under UV radiation, photogenerated electrons migrate from the conduction band of the ZnO to the CNTs phase which can enhance the lifetime of the charge separation state [63]. Therefore, CNT acts as photogenerated electron acceptor and an effective electron trapping site for ZnO, and can inhibit the rate of electron-hole recombination. In addition, it has been reported that PPy has low adsorption capacity, facilities on the photo-excited electron-hole separation, and makes the contact between photo-excited holes,  $^-\text{OH}$  and reactive oxygen species, thus facilitating the formation of  $^{\bullet}\text{OH}$  [64-66], which significantly responded more to the 4-CP and destroyed it faster.

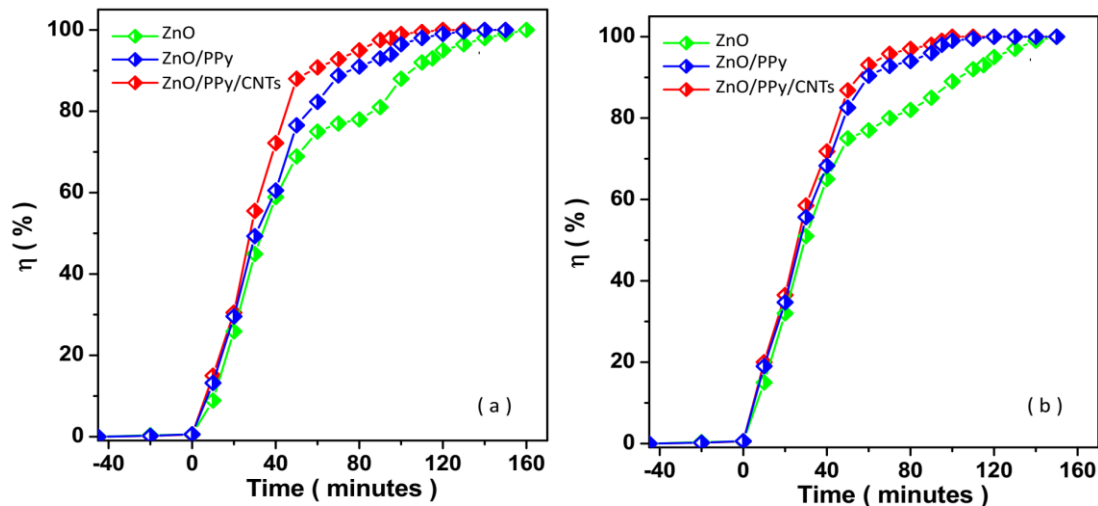


**Figure 5.** The photocatalytic degradation performance of ZnO, ZnO/PPy and ZnO/PPy/CNTs for removal of 100 ml of 6mg/l 4-CP in water under dark condition and the irradiation of (a) UV light and (b) simulated sunlight.

Figure 5b shows that after 60 minutes of simulated sunlight, the significant photodegradation is obtained and  $\eta$  values for ZnO, ZnO/PPy and ZnO/PPy/CNTs are determined as 77.0, 90.4 and 93.1 %, respectively. The 100% degradation of 4-CP for ZnO, ZnO/PPy and ZnO/PPy/CNTs is obtained after 150, 120 and 100 minutes of simulated sunlight, respectively. The fast degradation rate under simulated sunlight and the UV light irradiation is related to narrowing band gap of ZnO/PPy/CNTs,

which increases the visible range of optical absorption. As a result, PPy and CNTs have a favorable synergistic effect on ZnO's light harvesting capacity, which is beneficial for increased absorption on the surface of the composite photocatalyst, which boosts photocatalytic properties under visible light. Therefore, ZnO/PPy/CNTs were selected for further photodegradation studies of 4-CP under simulated sunlight.

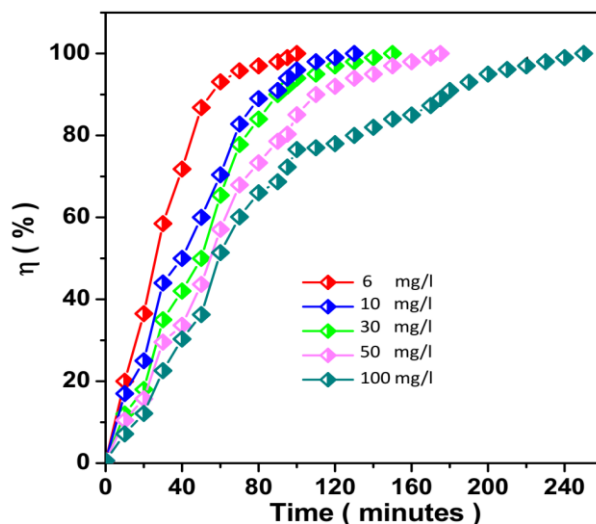


**Figure 6.** Photodegradation efficiency of the 100 ml of different 4-CP concentration (6, 10, 30, 50 and 100 mg/l) in presence of ZnO/PPy/CNTs under irradiation of simulated sunlight

Figure 6 shows the photocatalytic degradation performance of ZnO/PPy/CNTs for the removal of 100 ml of 6, 10, 30, 50 and 100 mg/l of 4-CP in water under the irradiation of simulated sunlight. It can be found that the 100% degradation of 6, 10, 30, 50 and 100 mg/l of 4-CP is obtained after 100, 130, 150, 175 and 250 minutes, respectively. In fixed amount of photocatalyst, as the initial 4-CP concentration increase, more 4-CP molecules are available for photodegradation which prevents the photocatalyst from utilizing the irradiated light to produce reactive species for degradation [67]. Moreover, the high concentration of 4-CP molecules scatters the light, inducing screening effects. These results are in agreement with the results of EIS and optical analyses.

The photocatalytic performance comparison between ZnO/PPy/CNTs and some other photocatalysts for degradation of 4-CP is summarized in Table 2. As seen, ZnO/PPy/CNTs exhibits the effective performance for photodegradation of 4-CP under simulated sunlight because of the positive synergistic effect of PPy and CNTs on the light harvesting ability of the ZnO which extends the absorption range of photocatalyst to the visible region, improves charge separation with the subsequent decrease in the recombination rate, and enhances the effective surface area of the photocatalyst.

The capability of the proposed photocatalyst was explored for degradation of 4-CP in the prepared real sample of wastewater. The photodegradation of 6 mg/l 4-CP prepared in deionized water and prepared in the real sample of textile wastewater were investigated using ZnO/PPy/CNTs under the irradiation of simulated sunlight. As seen from Figure 7, the 100% degradation of 4-CP solution prepared in deionized water and prepared in real sample of textile wastewater is obtained after 100 and 110 minutes, respectively. Thus, the degradation time for the sample prepared with real sample of

textile wastewater sample is higher than the sample prepared with deionized water, which can be related to the presence of various chlorophenolic compounds or additional 4-CP molecules in wastewater.

**Table 2.** The photocatalytic performance comparison between ZnO/PPy/CNTs and some other photocatalysts for degradation of 4-CP

| Photocatalyst  | 4-CP content (mg/l) | Light source          | Degradation time (minute) | $\eta$ (%) | Ref.      |
|--|---------------------|-----------------------|---------------------------|------------|-----------|
| ZnO/PPy/CNTs   | 100                 | Simulated sunlight    | 250                       | 100        | This work |
|  | 50                  |                       | 175                       |            |           |
|  | 30                  |                       | 150                       |            |           |
|  | 10                  |                       | 130                       |            |           |
|  | 6                   |                       | 100                       |            |           |
|  | 6                   | UV                    | 120                       | 100        |           |
| Sm, N, P-tridoped-TiO <sub>2</sub>                   | 400                 | Simulated sunlight    | 120                       | 87.13      | [21]      |
| Cu/ZnS   | 100                 | UV                    | 180                       | 100        | [22]      |
| TiO <sub>2</sub>                                     | 50                  | UV                    | 180                       | 82         | [25]      |
| graphite oxide                                       | 30                  | UV                    | 100                       | 92         | [23]      |
| graphene oxide                                       | 30                  | UV                    | 100                       | 97         | [23]      |
| Fe <sub>3</sub> O <sub>4</sub> /TiO <sub>2</sub> /Ag | 30                  | UV                    | 165                       | 97         | [26]      |
| Reduced graphene oxide /Se-ZnO                       | 15                  | UV                    | 105                       | 99.02      | [24]      |
| ZnO/Carbon xerogel                                   | 10                  | Solar & visible light | 300                       | 88         | [27]      |
| FeTiO <sub>3</sub> /TiO <sub>2</sub>                 | 6                   | UV                    | 180                       | 75         | [29]      |
| W-doped ZnO  | 5                   | Simulated sunlight    | 150                       | 95         | [28]      |

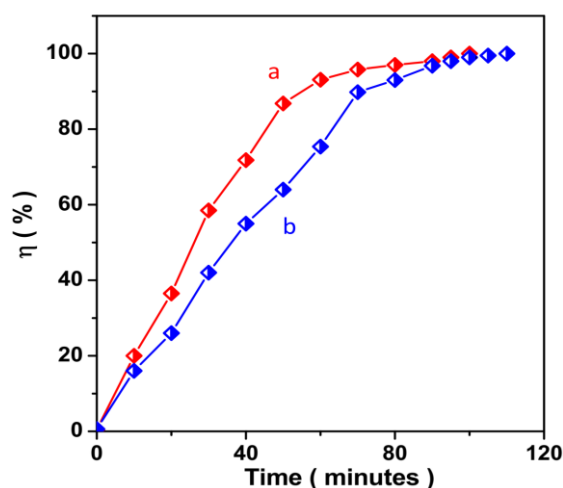


**Figure 7.** Photocatalytic degradation performance of ZnO/PPy/CNTs for remove of 100 ml of 6 mg/l of 4-CP (a) prepared in deionized water and (b) prepared in real sample of textile wastewater under irradiation of simulated sunlight.

#### 4. CONCLUSION

This study focused on the preparation of ZnO/PPy/CNTs nanocomposite using a facile solution method and application for photodegradation of 4-CP from wastewater under irradiation UV and simulated sunlight. Structural characterizations illustrated the successful formation of nanocomposites. EIS analysis indicated to low charge transfer resistance of ZnO/PPy/CNTs nanocomposite. Results of optical studies indicated that the  $E_g$  of ZnO, ZnO/PPy and ZnO/PPy/CNTs were estimated  $\sim 3.39$ ,  $3.30$  and  $3.17$  eV, respectively, and the values of the  $E_g$  of ZnO decreased slightly as the addition of PPy and CNTs to the ZnO structure. The photodegradation studies showed that ZnO/PPy/CNTs exhibited the effective photodegradation of 4-CP under simulated sunlight because of the positive synergistic effect of PPy and CNTs on the light harvesting ability of ZnO. Study of capability of the ZnO/PPy/CNTs for degradation of 4-CP in the prepared real sample of textile wastewater showed the proposed photocatalyst can effectively be used for the degradation of 4-CP from industrial wastewater.

#### ACKNOWLEDGEMENT

This work is supported by The Science and Technology Research Plan of Liaoning Province Education Department [LJKZ1064].

#### References

1. D. Ge, H. Yuan, J. Xiao and N. Zhu, *Science of The Total Environment*, 679 (2019) 298.
2. A. Bahrami, S. Jafarnejad, H. khoshnezhad Ebrahimi, S.M.M. Dezfouli and R. Pahlevani, *Systematic Reviews in Pharmacy*, 11 (2020) 905.
3. G. Li, S. Huang, N. Zhu, H. Yuan, D. Ge and Y. Wei, *Chemical Engineering Journal*, 421 (2021) 127852.
4. F. Chen, J. Ma, Y. Zhu, X. Li, H. Yu and Y. Sun, *Journal of Hazardous Materials*, 426 (2022) 128064.
5. H. Maleh, M. Alizadeh, F. Karimi, M. Baghayeri, L. Fu, J. Rouhi, C. Karaman, O. Karaman and R. Boukherroub, *Chemosphere*, (2021) 132928.
6. C. Shi, Z. Wu, F. Yang and Y. Tang, *Solid State Sciences*, 119 (2021) 106702.
7. K.A. Zahidah, S. Kakoei, M. Kermanioryani, H. Mohebbi, M.C. Ismail and P.B. Raja, *International Journal of Engineering and Technology Innovation*, 7 (2017) 243.
8. F. Husairi, J. Rouhi, K. Eswar, C.R. Ooi, M. Rusop and S. Abdullah, *Sensors and Actuators A: Physical*, 236 (2015) 11.
9. H.B.B. de Mesquita, G. Doornbos, D.A. van der Kuip, M. Kogevinas and R. Winkelmann, *American journal of industrial medicine*, 23 (1993) 289.
10. B. Bai, Q. Nie, H. Wu and J. Hou, *Powder Technology*, 394 (2021) 1158.
11. M. Khosravi, *Psychiatry*, 27 (2019) 171.
12. G. Li, H. Yuan, J. Mou, E. Dai, H. Zhang, Z. Li, Y. Zhao, Y. Dai and X. Zhang, *Composites Communications*, 29 (2021) 101043.
13. W. Liu, J. Li, J. Zheng, Y. Song, Z. Shi, Z. Lin and L. Chai, *Environmental Science & Technology*, 54 (2020) 11971.
14. M. Nazeer, F. Hussain, M.I. Khan, E.R. El-Zahar, Y.-M. Chu and M. Malik, *Applied Mathematics and Computation*, 420 (2022) 126868.
15. X. Yan, T. Zhu, X. Fan and Y. Sun, *Chemical Engineering Journal*, 245 (2014) 41.
16. T. Sankara Narayanan, G. Magesh and N. Rajendran, *Fresenius Environmental Bulletin*, 12 (2003)

17. M.Y. Ghaly, G. Härtel, R. Mayer and R. Haseneder, *waste management*, 21 (2001) 41.
18. A.T. Mohammad, M.A. Al-Obaidi, E.M. Hameed, B.N. Basheer and I.M. Mujtaba, *Journal of Water Process Engineering*, 33 (2020) 100993.
19. M.O. Azzam, M. Al-Tarazi and Y. Tahboub, *Journal of hazardous materials*, 75 (2000) 99.
20. E. Brillas, R. Sauleda and J. Casado, *Journal of the Electrochemical Society*, 145 (1998) 759.
21. H. Jiang, Q. Wang, S. Zang, J. Li and Q. Wang, *Journal of hazardous materials*, 261 (2013) 44.
22. W. Wang, G.-J. Lee, P. Wang, Z. Qiao, N. Liu and J.J. Wu, *Separation and Purification Technology*, 237 (2020) 116469.
23. K. Bustos-Ramírez, C.E. Barrera-Díaz, M. De Icaza-Herrera, A.L. Martínez-Hernández, R. Natividad-Rangel and C. Velasco-Santos, *Journal of Environmental Health Science and Engineering*, 13 (2015) 33.
24. S. Kumar, R.D. Kaushik and L.P. Purohit, *Separation and Purification Technology*, 275 (2021) 119219.
25. A. Payan, M. Fattahi and B. Roozbehani, *Journal of Environmental Health Science and Engineering*, 16 (2018) 41.
26. A. Shojaie, M. Fattahi, S. Jorfi and B. Ghasemi, *International Journal of Industrial Chemistry*, 9 (2018) 141.
27. N.P. de Moraes, R.B. Valim, R. da Silva Rocha, M.L.C.P. da Silva, T.M.B. Campos, G.P. Thim and L.A. Rodrigues, *Colloids and Surfaces A: Physicochemical and Engineering Aspects*, 584 (2020) 124034.
28. M. Aslam, M.T. Soomro, I.M. Ismail, N. Salah, M. Gondal and A. Hameed, *Journal of Environmental Chemical Engineering*, 3 (2015) 1901.
29. Y. Ma, J. Chen, Y. Wang, Y. Zhao, G. Zhang and T. Sun, *Research on Chemical Intermediates*, 47 (2021) 997.
30. B. Bai, S. Jiang, L. Liu, X. Li and H. Wu, *Powder Technology*, 387 (2021) 22.
31. X.-Q. Lin, Z.-L. Li, B. Liang, H.-L. Zhai, W.-W. Cai, J. Nan and A.-J. Wang, *Water research*, 162 (2019) 236.
32. M. Khosravi, *European Journal of Translational Myology*, 30 (2020) 9509.
33. J. Ahmed, M. Faisal, M. Jalalah, S. Alsareii and F.A. Harraz, *Journal of Electroanalytical Chemistry*, 898 (2021) 115631.
34. Y. Hui and S. Zhang, *International Journal of Electrochemical Science*, 16 (2021) 210635.
35. Y.-M. Chu, B. Shankaralingappa, B. Gireesha, F. Alzahrani, M.I. Khan and S.U. Khan, *Applied Mathematics and Computation*, 419 (2022) 126883.
36. N. Duc Vu Quyen, D. Quang Khieu, T.N. Tuyen, D. Xuan Tin and B. Thi Hoang Diem, *Journal of Chemistry*, 2019 (2019) 4260153.
37. R. Mosaddegh, S. Nabi, S. Daei, F. Mohammadi, G. Masoumi, S. Vaziri and M. Rezai, *Open access emergency medicine: OAEM*, 11 (2019) 205.
38. S. Sakthivel and A. Boopathi, *Journal of Chemistry and Chemical Sciences*, 4 (2014) 150.
39. H. Savaloni and R. Savari, *Materials Chemistry and Physics*, 214 (2018) 402.
40. P. Xu, L. Cui, S. Gao, N. Na and A.G. Ebadi, *Molecular Physics*, (2021) e2002957.
41. K. Eswar, J. Rouhi, H. Husairi, M. Rusop and S. Abdullah, *Advances in Materials Science and Engineering*, 2014 (2014) 1.
42. X. Qiu, Q. Hua, L. Zheng and Z. Dai, *RSC Advances*, 10 (2020) 5283.
43. M. Khosravi, *Current Psychology*, 40 (2021) 5735.
44. S. Vaziri, R. Mosaddegh, M. Rezai, F. Mohammadi and M.A. Ashari, *Journal of Critical Reviews*, 7 (2019) 2020.
45. W.H. Leng, Z. Zhang, J.Q. Zhang and C.N. Cao, *The Journal of Physical Chemistry B*, 109 (2005) 15008.
46. J. Rouhi, S. Mahmud, S. Hutagalung and S. Kakooei, *Micro & Nano Letters*, 7 (2012) 325.

47. I. Ahmad, M.S. Akhtar, E. Ahmed and M. Ahmad, *Separation and Purification Technology*, 245 (2020) 116892.
48. T.H. Zhao, M.I. Khan and Y.M. Chu, *Mathematical Methods in the Applied Sciences*, (2021) 1.
49. J. Rouhi, S. Kakooei, S.M. Sadeghzadeh, O. Rouhi and R. Karimzadeh, *Journal of Solid State Electrochemistry*, 24 (2020) 1599.
50. W. Kong, Y. Zhao, J. Xuan, Z. Gao, J. Wang, S. Tan, F. Jia, Z. Teng, M. Sun and G. Yin, *Applied Surface Science*, 537 (2021) 147998.
51. S. Zhang, H. Niu, Y. Lan, C. Cheng, J. Xu and X. Wang, *The Journal of Physical Chemistry C*, 115 (2011) 22025.
52. R. Hassanzadeh, A. Siabi-Garjan, H. Savaloni and R. Savari, *Materials Research Express*, 6 (2019) 106429.
53. Z. Zhang, Y. Yang and D. Cheng, *International Journal of Electrochemical Science*, 16 (2021) 21115.
54. B. Han, X. Wei and R. Gu, *International Journal of Electrochemical Science*, 16 (2021) 210618.
55. M. Chougule, S. Sen and V. Patil, *Journal of Applied Polymer Science*, 125 (2012) E541.
56. R. Kandulna and R. Choudhary, *Optik*, 144 (2017) 40.
57. M.A. Chougule, G.D. Khuspe, S. Sen and V.B. Patil, *Applied Nanoscience*, 3 (2013) 423.
58. A. Benyounes, N. Abbas, M. Hammi, Y. Ziat, A. Slassi and N. Zahra, *Applied Physics A*, 124 (2018) 1.
59. A. Murali, P.K. Sarswat and M.L. Free, *Environmental Science and Pollution Research*, 27 (2020) 25042.
60. T. Su, Q. Shao, Z. Qin, Z. Guo and Z. Wu, *Acs Catalysis*, 8 (2018) 2253.
61. P. Karimian and M.A. Delavar, *Pakistan Journal of Medical & Health Sciences*, 14 (2020) 1405.
62. P. Sehgal and A.K. Narula, *Optical Materials*, 79 (2018) 435.
63. I.E. Oliveira, R.M. Silva, A.V. Girão, J.L. Faria, C.G. Silva and R.F. Silva, *European Journal of Inorganic Chemistry*, 2020 (2020) 1743.
64. S. Silvestri, C.D. Ferreira, V. Oliveira, J.M. Varejão, J.A. Labrincha and D.M. Tobaldi, *Journal of Photochemistry and Photobiology A: Chemistry*, 375 (2019) 261.
65. Y.-M. Chu, U. Nazir, M. Sohail, M.M. Selim and J.-R. Lee, *Fractal and Fractional*, 5 (2021) 119.
66. S.M.M. Dezfouli and S. Khosravi, *Indian Journal of Forensic Medicine and Toxicology*, 15 (2021) 2674.
67. C.M. Kgoetlana, S.P. Malinga and L.N. Dlamini, *Catalysts*, 10 (2020) 699.